

## TESTING OF THE DELAY TIME OF WIRELESS COMMUNICATION OF CNC MACHINE TOOLS' PROBES AND CONTROLLER

Michał Jankowski, Adam Woźniak

Warsaw University of Technology, Faculty of Mechatronics, Św. A. Boboli 8, 02-525 Warsaw, Poland  
(✉ [M.Jankowski@mchtr.pw.edu.pl](mailto:M.Jankowski@mchtr.pw.edu.pl), +48 535 533 666, [A.Wozniak@mchtr.pw.edu.pl](mailto:A.Wozniak@mchtr.pw.edu.pl))

### Abstract

Touch-trigger probes for CNC milling machines usually use wireless communication in the radio or IR band. Additionally they enable triggering signal filtering in order to avoid false triggers of the probe. These solutions cause a delay in trigger signal transmission from the probe to the machine tool controller. This delay creates an additional pre-travel component, which is directly proportional to the measurement speed and which is the cause of a previously observed but not explained increase of the pre-travel with the increase of the measurement speed. In the paper, a method of testing the delay time of triggering signal is described, an example of delay time testing results is presented and the previous, unexplained results of other researchers are analysed in terms of signal transmission delay.

Keywords: probes, CNC machine tools, communication delay, measurement speed.

© 2018 Polish Academy of Sciences. All rights reserved

## 1. Introduction

The probes for CNC machine tools are measurement devices mounted in a tool – in its spindle or turret, depending on the machine type. They are widely used for the setting and inspection of a workpiece. Moreover, they can be used for determination of the machine tool's kinematic errors [1–9]. That is why – in general – the probe's errors (including wireless communication) influence the accuracy of machining.

Opposite to the probes for coordinate measuring machines, whose performance is well-known [10–12] and which usually work in a laboratory environment, the probes for CNC machine tools work in a harsh, production environment. This increases the risk of false triggers. To avoid them, a signal from the probe transducer to the machine tool controller can be filtered. It can be necessary especially in the case of ultra-precise strain gauge probes which are much more vibration-sensitive than common kinematic probes. However, the trigger signal filtration is used also in kinematic probes and even in such probes filtering times can be set up to several dozen of milliseconds. In such a case there is a significant delay between the detection of contact of the stylus tip with the measured surface and the appearance of the trigger signal at the filter output.

It was assumed that the delay resulting from the signal filtering can be increased by a delay caused by a wireless communication system [13]. Such communication is commonly used in

probes for CNC milling machines, because in these machines probes are mounted in the spindle which can rotate.

The abovementioned delay affects the pre-travel and the triggering radius of the probe. A pre-travel  $w$  is a displacement of the stylus tip in a given direction required to trigger the probe. This parameter is easy to use in the mechanical modelling of the probes, but in real measurements a neutral position of the stylus tip is not known. That is why another parameter, a triggering radius  $r$ , was proposed. For a given direction it is equal to the distance between the triggering point – the stylus tip position corresponding to triggering of the probe – and the centre of best-fitted element determined by using triggering points for all used directions.

During measurements, when the probe is triggered, its transducer generates a trigger signal. If this signal is being filtered and transmitted, the machine axes keep moving, so when the probe trigger is detected by the machine tool controller, the position of the probe is different from its position when the transducer of the probe detects the measured surface. This displacement increases the probe pre-travel according to the equation [14]:

$$w(\alpha, \beta) = w_T(\alpha, \beta) + w_I(\alpha, \beta) = w_T(\alpha, \beta) + v\tau, \quad (1)$$

where  $\alpha$  and  $\beta$  – a pair of angles defining the measurement direction;  $w$  – an overall pre-travel;  $w_T$  – a pre-travel component depending on the probe transducer;  $w_I$  – a pre-travel component depending on the trigger signal transmission delay;  $v$  – a measurement speed;  $\tau$  – a delay time.

The described linear relationship of the pre-travel and the measurement speed is shown in [15]. In this research the measurement speed was changed from 50 mm/min to 1250 mm/min. The corresponding pre-travel changes were:

- i) for a 55 mm stylus from about 0.020 mm to about 0.115 mm;
- ii) for a 95 mm stylus from about 0.030 mm to about 0.140 mm.

In both cases the pre-travel change seems to be proportional to the measurement speed change what supports the hypothesis that the pre-travel increase is caused by the delay in trigger signal transmission.

The aim of research presented in this paper was to determine if the delay caused by the CNC machine tool probe – controller wireless communication or the delay caused by trigger signal filtering is dominant. To achieve this goal the delay between triggering the probe transducer and the appearance of the trigger signal on the probe interface output was measured for 3 probes and for various trigger filter settings, using a dedicated setup for probe testing. Additionally, the delay was determined for 1 probe on a machine tool, using a gauge ring.

## 2. Delay time testing method

### 2.1. General principle

To test the delay time  $\tau$  – the delay between triggering the probe transducer and appearing the trigger signal on the probe interface output – it was assumed that a mean triggering radius for all measurement directions  $\bar{r}$  – the mean of all the triggering radius  $r$  values obtained for a single probe for various measurement directions – is equal to a mean pre-travel for all measurement directions  $\bar{w}$  – the mean of all of the pre-travel  $w$  values obtained for a single probe for various directions.

Next, for every tested probe and for every tested trigger filter setting a mean measured triggering radius for all measurement directions  $\overline{mr}$  – the sum of the mean triggering radius for all measurement directions  $\bar{r}$  and a constant value depending on the measurement method – was

measured for several measurement speeds. For the measurements performed using the dedicated setup, 4 measurement speeds were used:

- i) 0.17 mm/s (10 mm/min);
- ii) 0.50 mm/s (30 mm/min);
- iii) 0.83 mm/s (50 mm/min);
- iv) and 1.17 mm/s (70 mm/min).

For the measurements performed on the machine tool, 3 measurement speeds were used:

- i) 0.83 mm/s (50 mm/min);
- ii) 1.67 mm/s (100 mm/min);
- iii) 2.50 mm/s (150 mm/min).

Assuming that factors other than the trigger signal transmission delay have a negligible influence on the change of the mean triggering radius value for all measurement directions  $\overline{mr}$ , a slope of regression line calculated for all of the obtained  $\overline{mr}$  values in a function of the measurement speed is equal to the delay time  $\tau$  value (in ms, if the  $\overline{mr}$  is in  $\mu\text{m}$  and the measurement speed  $v$  is in mm/s).

## 2.2. Triggering radius measurement method using dedicated setup

Triggering radii of the tested probes were measured using the moving master artefact method [16]. The general principle of this method is shown in Fig. 1. The stylus tip (1) of an immobilized tested probe (2) is placed in the centre of a master artefact (3) – a ring gauge or an inner hemisphere master artefact. The master artefact is fixed to a piezoelectric XYZ stage (4) which is used to displace the master artefact in various directions. These displacements cause triggering of the probe. Every time the probe is triggered, the actual X, Y and Z coordinates of the master artefact are read from the displacement sensors of the piezoelectric stage. Each set of values of these coordinates gives one triggering point  $TG_i$ , where  $i$  is a number assigned to the tested measurement direction.

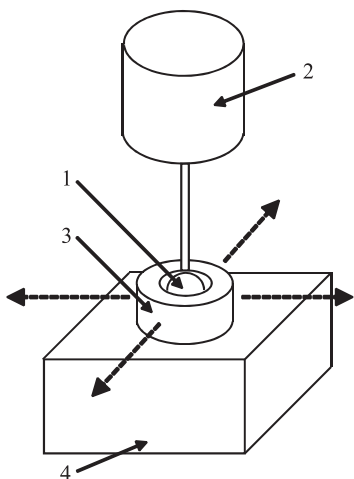


Fig. 1. A scheme of the moving master artefact method: 1 – the stylus tip of the tested probe; 2 – the tested probe; 3 – the master artefact – a ring gauge or inner hemisphere master artefact, 4 – the piezoelectric XYZ stage.

After execution of the master artefact displacements in all of the tested measurement directions, the obtained triggering points  $TG_i$  are used to determine the best-fitted element – a circle or a sphere. A distance between the centre of this element  $O_S$  and the triggering point  $TG_i$  is a

measured triggering radius in  $i$  direction  $mr_i$  – the sum of the triggering radius  $r_i$  in  $i$  direction and the difference between the radii of the master artefact and the stylus tip:

$$mr_i = r_i + (r_G - r_{ST}), \tag{2}$$

where  $r_G$  – a radius of the master artefact;  $r_{ST}$  – a radius of the stylus tip. A graphical interpretation of the abovementioned radii is shown in Fig. 2.

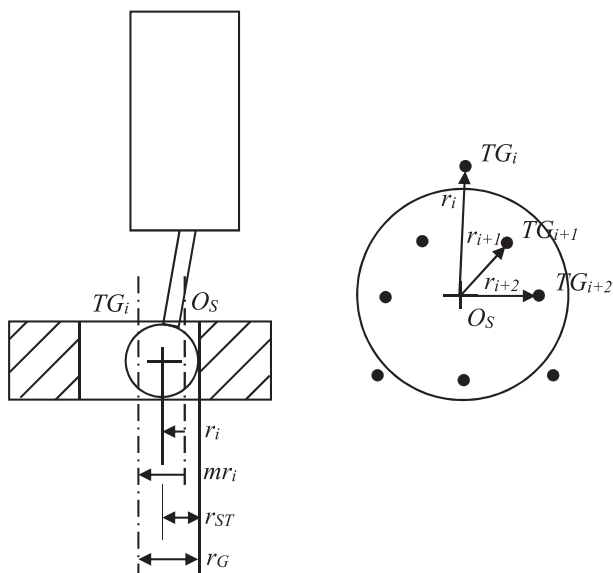


Fig. 2. The triggering and measured triggering radii:  $TG_i$  – the point corresponding to triggering of the probe;  $O_S$  – the centre of best-fitted element determined for all points  $TG$ ;  $mr_i$  – the measured triggering radius in direction  $i$ ,  $r_i$  – the triggering radius in direction  $i$ ,  $r_G$  – the radius of the gauge;  $r_{ST}$  – the radius of the stylus tip.

The mean triggering radius for all measurement directions  $\bar{r}$  is the mean value of all of the  $r_i$  values obtained during the test (for a given probe, given probe settings and a given measurement speed).

The test setup implementing the moving master artefact method was described in [13]. It uses a Physik Instrumente P-615.3CD NanoCube as the XYZ stage. The stage controller communicates with a PC by a National Instruments NI USB-6259 BNC data acquisition card and the measurement is controlled by a computer program developed in LabVIEW environment.

The master artefact used in this research was a ring gauge. Its diameter  $D_T$  was 6.0181 mm. While all tested probes were equipped with the same stylus with a tip diameter of 5.9999 mm, the difference between the mean measured triggering radius for all measurement directions  $\overline{mr}$  and the mean triggering radius for all measurement directions  $\bar{r}$  equals 9.1  $\mu\text{m}$ .

However, despite the fact that the triggering radius values can be easily calculated, it was decided to work on the measured triggering radius values in order to avoid taking into account uncertainties of measurement of the master artifact and the stylus tip diameters.

The extended uncertainty (for coverage factor  $k = 2$ ) of the mean measured triggering radius for all measurement directions  $\overline{mr}$  determined using the described setup was calculated in [13] and it is equal to 0.034  $\mu\text{m}$ . However, in the research described in [13] the measurements were

performed using an inner hemisphere master artefact and the probes were tested in 325 directions. In this research the probes were tested in only 36 directions, so the extended uncertainty is  $\sqrt{325}/\sqrt{36}$  times greater. Hence,  $U(\overline{mr}) = 0.103 \mu\text{m}$ .

In order to minimize the influence of random errors, for every probe, every filter setting and every measurement speed 10 measurements of  $\overline{mr}$  were performed. Hence, for every case the mean  $\overline{mr}$  value was determined with an extended ( $k = 2$ ) uncertainty of  $0.033 \mu\text{m}$ . The results obtained using the described setup correspond to the results which would be obtained by a measurement of the gauge ring using a machine tool, but the setup has a much better accuracy than an average machine tool.

### 2.3. Triggering radius measurement method using gauge ring

To test the probe on a Haas VF8 machine tool, a gauge ring was used. Its diameter was 52.001 mm. It was measured in 36 directions with a step of  $10^\circ$ . The longer the triggering radius in a given direction was, the longer the measured radial distance in this direction was. In this method the measured radius is equal to:

$$mr_i = r_i - (r_{STr} - r_{STnom}), \quad (3)$$

where  $r_{STr}$  – a real stylus tip radius and  $r_{STnom}$  – a nominal stylus tip radius.

In order to minimize the influence of random errors, for every measurement speed 5 measurements of  $\overline{mr}$  were performed.

## 3. Experimental results

To determine if the delay time caused by the CNC machine tool probe – controller wireless communication or the delay caused by trigger signal filtering is dominant, three popular probes have been used. One of them is a Renishaw OMP60 probe which trigger filter can be turned off or set to 10 ms, 20 ms or 40 ms. The remaining two probes are Renishaw OMP40-2 compact probes which trigger filter can be only turned off or turned on. One of the OMP40-2 probes was heavily used, while the other was not. All tested probes were working with the same Renishaw OMI optical interface and were equipped with a 50 mm long stylus. The probe tested on the machine tool was a Renishaw OMP40-2 probe equipped with a 100 mm long stylus. This probe was tested only for the filter turned on. The results of delay time measurement for OMP60 as well as for OMP40-2 probes are collected in Tables 1 and 2, respectively. The mean measured triggering radius for all measurement directions vs. the measurement speed and filter settings for OMP60 and for OMP40-2 probes are presented in Fig. 3 and Fig. 4, respectively.

For the Renishaw OMP60 probe it was observed that, if the filter was turned on, the mean measured triggering radius increased with increasing of the measurement speed and this increasing was greater when a longer filtering time was set.

However, if the filter was turned off, the mean triggering radius decreased with increasing of the measurement speed. It means that the delay time in this case was negligible ( $\approx 0$ ) and that other factors influencing mean triggering radius value existed.

These factors probably exist also if the filter is turned on. That is why for every measurement speed the difference between the mean  $\overline{mr}$  value for the filter turned off and the intercept value of regression line for the filter turned off was calculated. Next, by subtracting the calculated difference values from all (for every filter setting, but only for a given measurement speed) of the

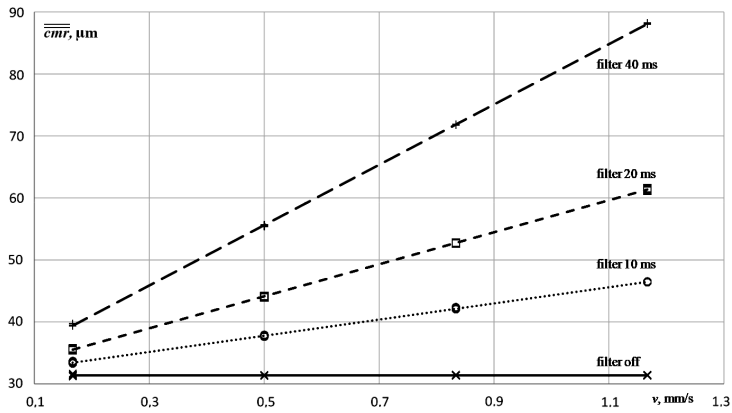


Fig. 3. The corrected mean measured triggering radius for all measurement directions vs. the measurement speed and filter settings for the OMP60 probe.

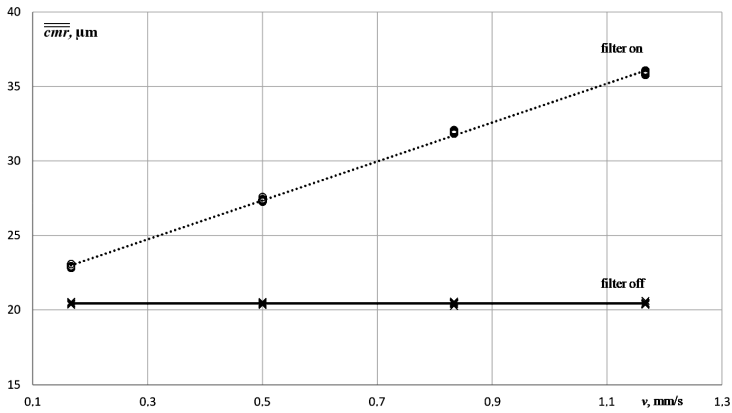


Fig. 4. The corrected mean measured triggering radius for all measurement directions vs. the measurement speed and filter settings for the rarely used OMP40-2 probe.

obtained  $\overline{cmr}$  values, the corrected mean measured triggering radii for all measurement directions  $\overline{cmr}$  values were calculated.

The delay time for various filter settings was determined by calculation of the slope of corresponding simple regression line for  $\overline{cmr}$  values. These results are presented in Table 1, while the obtained  $\overline{cmr}$  values are shown in Fig. 3.

Table 1. Results of delay time measurement for the OMP60 probe.

Filter	Corrected delay time, ms
off	$\approx 0$
10 ms	13.0
20 ms	25.8
40 ms	48.7

It has to be clearly stated that the corrected values of mean measured triggering radius are not real values. The real values are the values before correction. The corrected values were calculated only for a better determination of the delay time, while in reality all the non-delay-related effects still existed.

As it can be seen, the calculated delay times are slightly longer than the corresponding nominal trigger signal filtering times. In the case of this probe, the wireless communication with the interface receiver has a negligible influence on the pre-travel of the probe. Additionally, the influence of non-delay-related factors has been observed, but it is much smaller than the influence of filter-caused delay.

For the tested OMP40-2 probes, both the rarely used one and the heavily used one, the same effect as for the OMP60 probe was observed. If the filter was turned on, the mean measured triggering radius increased with increasing of the measurement speed. The values of corrected mean triggering radius for the rarely used probe are presented in Fig. 4. After the correction had been performed, the delay times for both OMP40-2 probes were determined. The obtained values for the rarely used probe are presented in Table 2, while the results for the heavily used probe are shown in Table 3.

Table 2. Results of delay time measurement for the rarely used OMP40-2 probe.

Filter	Corrected delay time, ms
off	≈ 0
on	13.1

Table 3. Results of delay time measurement for the heavily used OMP40-2 probe.

Filter	Corrected delay time, ms
off	≈ 0
on	12.9

As it can be seen, the delay time values determined for both OMP40-2 probes with the filter turned on are very similar to the values obtained for the OMP60 probe with the filter set to 10 ms – the same before and after correction eliminating the influence of non-delay-related effects. The described above results clearly show that also for OMP40-2 type probes, in the case of delay time, the influence of wireless communication itself is negligible in comparison with the influence of the trigger signal filtering.

In the previous research the influence of the optical interface type and the optical transmission method was observed [13]: the OMP40-2 probe working with an OMI interface had a delay time of 13.0 ms, while the same probe working with an OMI-2 interface had a delay time of 13.5 ms. What is more, the previous research shown that the radio probes can cause a significant delay in trigger signal transmission even if the trigger filter is disabled [13]. The issue requires further tests.

The measured mean triggering radius values obtained on the machine tool are shown in Fig. 5. Additionally, the measured triggering radius characteristics are shown in Fig. 6. The delay value obtained for this probe is equal to 14.5 ms and is slightly greater than the delay values obtained in measurements performed using the dedicated setup. This is probably an effect of an additional delay resulting from the machine tool controller operation.

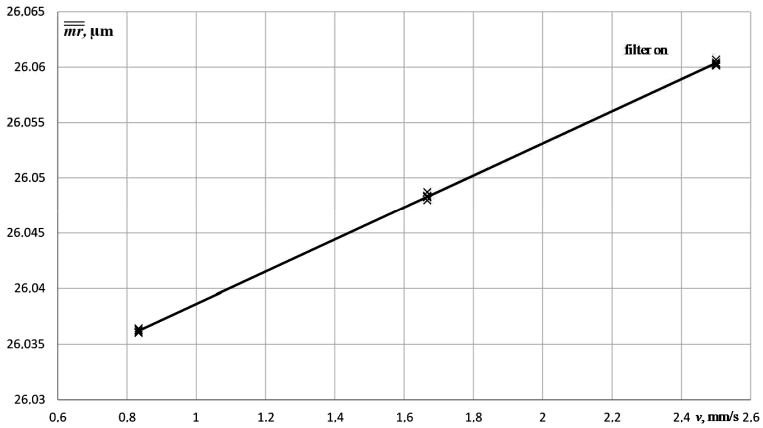


Fig. 5. The mean measured triggering radius for all measurement directions vs. the measurement speed and filter settings for the OMP40-2 probe tested on the machine tool.

As it can be seen, the shape of triggering radius characteristic is constant, but the offset resulting from the higher measurement speed is clearly visible. The triggering radius variation – a parameter corresponding to the systematic error of the probe – is equal to 21  $\mu\text{m}$  for the

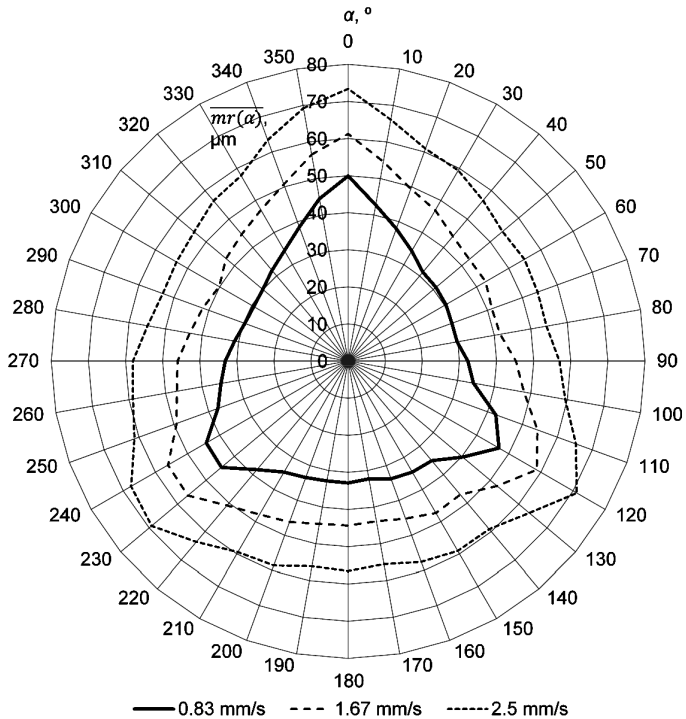


Fig. 6. The measured triggering radius characteristics for various measurement speed values for the OMP40-2 probe tested on the machine tool.

measurement speeds of 50 mm/min and 100 mm/min, and is equal to 20  $\mu\text{m}$  for the measurement speed of 150 mm/min. The offset value corresponding to the increase of measurement speed by 50 mm/min is about 12  $\mu\text{m}$  – more than a half of the triggering radius variation.

#### 4. Conclusions

Three optical, kinematic probes were tested in order to determine if the wireless communication itself or the trigger signal filtering has the dominant influence on the trigger signal transmission delay time. It was concluded that the influence of the wireless communication itself is negligible in comparison with the influence of the trigger signal filtering. The delay caused by the signal filtering is strongly dependent on the filter settings – at least in the case of the tested probes; it seems to be proportional to the nominal filtering time, but slightly – by about one fifth – greater.

However, the conclusion concerning the dominant role of trigger signal filtering in the signal transmission delay is limited to the optical probes – the previous research results suggest that communication in the radio band can be slower than the optical communication.

Moreover, further research is needed to answer the question whether different transmission methods are associated with different delay times.

#### References

- [1] Erkan, T., Mayer, J.R.R., Dupont, Y. (2011). Volumetric distortion assessment of a five-axis machine by probing a 3D reconfigurable uncalibrated master ball artefact. *Prec. Eng.*, 35(1), 116–125.
- [2] Mayer, J.R.R. (2012). Five-axis machine tool calibration by probing a scale enriched reconfigurable uncalibrated master balls artifact. *CIRP Ann. – Manuf. Techn.*, 61, 515–518.
- [3] Ibaraki, S., Iritani, T., Matsushita, T. (2013). Error map construction for rotary axes on five-axis machine tools by on-the-machine measurement using a touch-trigger probe. *Int. J. Mach. Tool. Manu.*, 68, 21–29.
- [4] Ibaraki, S., Ota, Y. (2013). Error calibration for five-axis machine tools by on-the-machine measurement using a touch-trigger probe. *International Journal of Automation Technology*, 8(1), 20–27.
- [5] Alami Mchichi, N., Mayer, J.R.R. (2014). Axis location errors and error motions calibration for a five-axis machine tool using the SAMBA method. *Proc. CIRP*, 14, 305–310.
- [6] Guiassa, R., Mayer, J.R.R., Balazinski, M., Engin, S., Delorme, F.E. (2014). Closed door machining error compensation of complex surfaces using the cutting compliance coefficient and on-machine measurement for a milling process. *Int. J. Comp. Integ. M.*, 27(11), 1022–1030.
- [7] Jiang, Z., Bao, S., Zhou, X., Tang, X., Zheng, S. (2015). Identification of location errors by a touch-trigger probe on five-axis machine tools with a tilting head. *Int. J. Adv. Manuf. Tech.*, 81(1), 149–158.
- [8] Mayer, J.R.R., Rahman, M.M., Łoś, A. (2015). An uncalibrated cylindrical indigenous artefact for measuring inter-axis errors of a five-axis machine tool. *CIRP Ann – Manuf. Techn.*, 64(1), 487–490.
- [9] Rahman, M.M., Mayer, R. (2016). Calibration performance investigation of an uncalibrated indigenous artefact probing for five-axis machine tool. *J. Mach. Eng.*, 16(1), 33–42.
- [10] Śladek, J. (2016). *Coordinate Metrology. Accuracy of Systems and Measurements*. Berlin: Springer-Verlag.
- [11] Śladek, J., Gaška, A. (2012). Evaluation of coordinate measurement uncertainty with use of virtual machine model based on Monte Carlo method. *Measurement*, 45(6), 1564–1575.

- [12] Dobosz, M., Woźniak, A. (2003). Metrological feasibilities of CMM touch trigger probes. Part II. experimental verification of the 3D theoretical model probe pretravel. *Measurement*, 34(4), 287–299.
- [13] Woźniak, A., Jankowski, M. (2016). Wireless communication influence on CNC machine tool probe metrological parameters. *Int. J Adv. Manuf. Technol.*, 82(1), 535–542.
- [14] Jankowski, M., Woźniak, A. (2016). Mechanical model of errors of probes for numerical controlled machine tools. *Measurement*, 77, 317–326.
- [15] Bohan, Z., Feng, G., Yan, L. (2015). Study on Pre-travel Behaviour of Touch Trigger Probe under Actual Measuring Conditions. *Proc. CIRP*, 27, 53–58.
- [16] Jankowski, M., Woźniak, A. (2014). Machine tool probes testing using a moving inner hemispherical master artefact. *Prec. Eng.*, 38(2), 421–427.